Indonesian Physical Review
Volume 09 Issue 03, September 2026
P-ISSN: 2615-1278, E-ISSN: 2614-7904

Characteristics of Mamuju City Urban Heat Island Based on Air Temperature and Landsat 8/9 Imagery

Abdul Rajab[1*], Pariabti Palloan[1], Agus Susanto[1], Adi Prasetyo[1]
[1] *Department of Physics, Faculty of Mathematics and Natural Sciences, Makassar State University, Indonesia*

Corresponding Author's E-mail: abdulrajab019@gmail.com

Article Info

Article info:
Received: 15-04-2026
Revised: 04-06-2026
Accepted: 06-07-2026

Keywords:
Urban Heat Island; Mamuju; Land Surface Temperature; Landsat; ERA5; Land Cover.

How To Cite:
A. Rajab, P. Palloan, A. Susanto, A. Prasetyo, "Characteristics of Mamuju City Urban Heat Island Based on Air Temperature and Landsat 8/9 Imagery", Indonesian Physical Review, vol. 9, no. 3, p 452-468, 2026.

DOI:
https://doi.org/10.29303/ipr.v9i3.679.

Abstract

Rapid urbanization in Mamuju City, Indonesia, has altered land cover patterns and contributed to the development of Urban Heat Island (UHI) conditions. This study aims to analyze the spatial and temporal characteristics of UHI in Mamuju City during the dry season (June–September) from 2015 to 2024, and to examine the relationships between land surface temperature, land cover change, and atmospheric temperature. The study integrates ERA5 reanalysis air temperature data with Landsat 8/9 Level-2 imagery using the Google Earth Engine platform. Land cover classification was conducted using the Random Forest algorithm with 200 decision trees, incorporating spectral bands, spectral indices (NDVI and NDBI), and topographic variables. Land Surface Temperature (LST) was derived from Landsat thermal data. UHI intensity was calculated as the difference between mean LST of built-up and bare land areas (urban zone) and the mean LST of vegetated, agricultural, and water areas (rural zone). Pearson correlation analysis was applied on a per-year basis to assess relationships between LST, NDVI, NDBI, and ERA5 air temperature. The results show that UHI intensity remained in the strong category (ΔT = 5.1–7.6°C) throughout the study period. Mean LST increased from 30.6°C in 2015 to 32.1°C in 2024, accompanied by a 69.2% increase in built-up area and a 7.9% decrease in dense vegetation. Land cover classification achieved an overall accuracy of 72.0% with a Kappa coefficient of 0.65. LST showed a positive correlation with NDBI (r = 0.662–0.721) and a negative correlation with NDVI (r = −0.658 to −0.693). ERA5 air temperature showed a weak and statistically insignificant correlation with LST (r = 0.137, p = 0.707). These results indicate that observed surface temperature patterns in Mamuju City are closely associated with land cover composition and change, while coarse-resolution reanalysis data are not suitable for representing intra-urban thermal variability at the city scale.

Introduction

Mamuju is a rapidly growing city whose urbanization has been driven by its status as the capital of West Sulawesi Province, established in 2004. Over two decades, residential areas, commercial zones, and road infrastructure have expanded rapidly, replacing natural vegetation and open land. According to the Central Bureau of Statistics of West Sulawesi

Province [1], the population of Mamuju Regency in 2014 was 265,234. This number increased to 289,453 by the end of 2023 [2]. These dynamic drivers drive high demand for housing and urban infrastructure, leading to the expansion of impervious surfaces such as concrete, asphalt, and metal roofing, which reduces natural heat dissipation and increases thermal energy accumulation. For comparison, a study by Atsidiqi et al. [3] in Kolaka confirms that urban sprawl intensifies UHI.

An Urban Heat Island (UHI) is a phenomenon in which surface and air temperatures in urban areas are higher than in surrounding regions. This condition increases building cooling loads, degrades air quality, and elevates heat stress risk for residents, particularly vulnerable groups [4]. while also reducing the efficiency and service life of critical urban infrastructure [5]. Mamuju's coastal plain location and humid tropical climate intensify solar radiation absorption, making it especially susceptible to heat accumulation. Research by Marsitha et al. [6] found that Mamuju has the highest frequency of thermal discomfort in Sulawesi, with 24.7% of days per year in the uncomfortable category. Global phenomena such as ENSO further amplify this condition, as reduced precipitation and heightened evaporation during El Niño events increase UHI intensity and diminish thermal comfort [7],[8].

The impacts of global climate change and local urbanization are clearly visible in the land-cover transformation of Mamuju City over the past decade. Wali et al. [9] showed that after the provincial division, Mamuju experienced the most intensive physical development escalation in West Sulawesi, marked by massive conversion of non-built-up land into functional urban areas. A similar pattern also occurs in Cirebon City, where the lack of green open space and the dominance of built-up land contribute to an increase in surface temperature of up to 3°C between the urban and suburban areas [10]. In Java Island, urbanization increases the intensity of the surface urban heat island (SUHI) by up to 5.97°C in Jakarta and 5.96°C in Bandung-Cimahi [11].

Setiawan et al. [12] state that small cities in Indonesia experience higher rates of temperature increase than metropolitan cities, often due to infrastructure growth without UHI mitigation. In recent studies, machine learning-based approaches, particularly the Random Forest algorithm implemented within Google Earth Engine, have demonstrated strong performance in urban land cover classification using Landsat imagery [13]. Such approaches have also proven effective for analyzing the relationship between land cover and surface temperature, as applied in Imola, Italy, where NDBI and NDVI indices were the dominant factors influencing LST variability [14]. Similarly, the use of the Random Forest algorithm on a cloud computing platform successfully mapped land cover in Bangkalan Regency with an accuracy of 91.39% [15].

This study makes two primary contributions. First, it provides the first spatially explicit, multi-temporal UHI characterization for Mamuju City, a rapidly growing urbanizing provincial capital in eastern Indonesia that remains underrepresented in the urban climate literature dominated by large Javanese cities. Second, by incorporating ERA5 reanalysis alongside Landsat-derived LST, this study empirically examines whether coarse-resolution atmospheric reanalysis data can serve as a proxy for local surface temperature dynamics in a secondary tropical city, a methodological question with direct implications for UHI monitoring in data-scarce regions.

The absence of a spatial UHI map for Mamuju City is a serious obstacle to the development of evidence-based adaptation policies. This study aims to fill a literature gap on UHI in Mamuju

City by integrating two data sources: air temperature from the ERA5 Reanalysis, which offers temporal reliability and has been applied in tropical urban studies in Indonesia [16], and multispectral satellite imagery, which enables broad-scale surface temperature mapping. The combination of these two data sources enables a more comprehensive analysis of UHI, from temperature distribution maps to diurnal and seasonal variations, to support sustainable, healthy urban planning for the community.

Experimental Method

This study employs a quantitative, descriptive-analytical approach. This research is spatiotemporal, analyzing the distribution and patterns of UHI across space and time. This approach enables the integration of surface temperature data and air temperature data, making the research results more comprehensive and classifiable into local climate zones to support spatial planning and UHI mitigation [17].

The study area includes Mamuju District and Simboro District, which were selected because they represent the city center area with high urbanization rates and significant land cover changes. Administratively, this area is bordered by the Makassar Strait and Kalukku District to the north, the Makassar Strait to the west, Tapalang and Tapalang Barat Districts to the south, and Kalukku District and Mamasa Regency to the east (Figure 1).

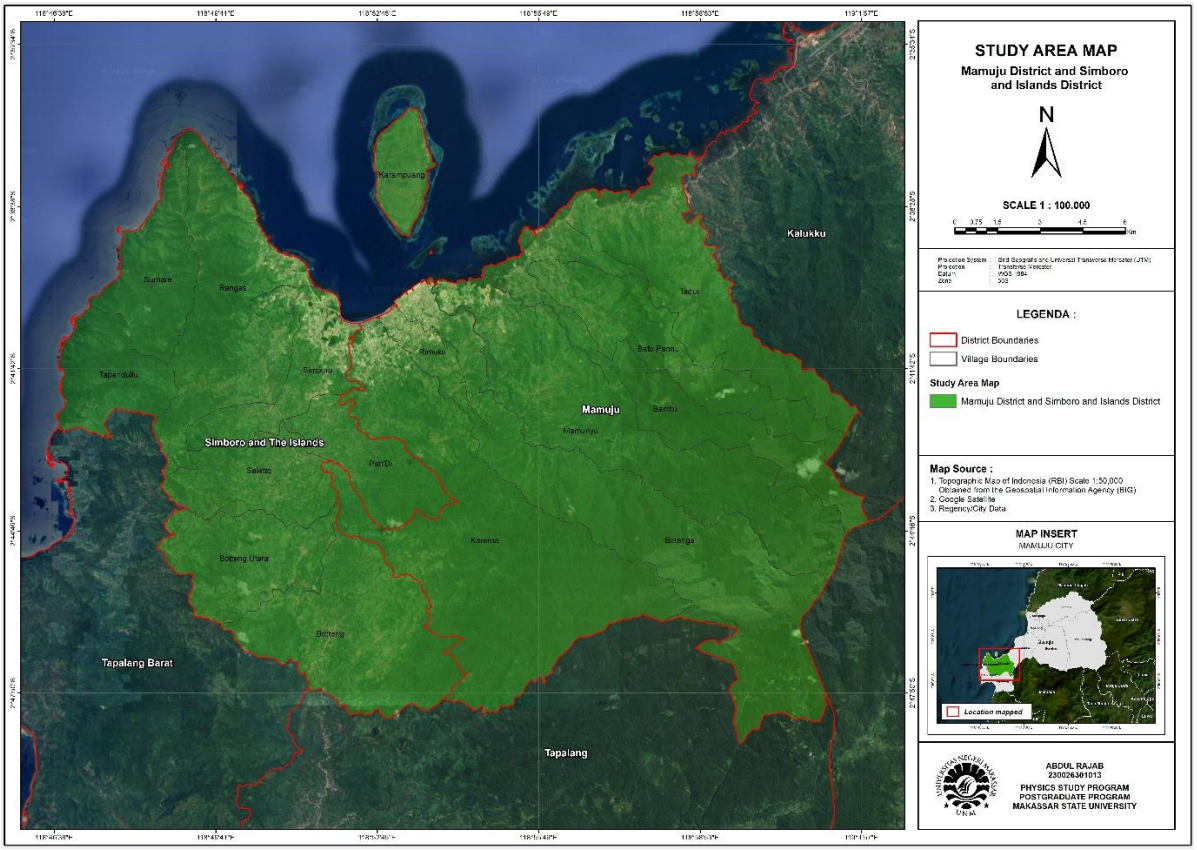

Figure 1. Map of the Mamuju City study area, 2025

This study utilized two main data sources. First, air temperature data from ERA5 Reanalysis, a global atmospheric reanalysis product from the European Center for Medium-Range Weather Forecasts (ECMWF), with a spatial resolution of 0.25° × 0.25° and a temporal

resolution of 1 hour, using the air temperature parameter at 2 meters above ground level[16],[18]. In this study, ERA5 serves a comparative analytical role: it provides an independent atmospheric temperature baseline against which Landsat-derived LST is assessed, enabling evaluation of whether coarse-resolution reanalysis data can represent local surface thermal dynamics in a secondary tropical city. ERA5 data have been extensively validated and are highly reliable for urban climate applications [11]. The data were downloaded from the Copernicus Climate Data Store in NetCDF format.

Second, Landsat 8/9 Collection 2 Level-2 imagery obtained from the USGS EarthExplorer with a cloud cover filter of less than 10%. Restricting analysis to Landsat 8 and 9 sensors ensures radiometric consistency throughout the 2015–2024 period, avoiding inter-sensor calibration uncertainties. Both datasets focused on the dry season (June–September) from 2015 to 2024 to maintain consistency in analysis and minimize interference from cloud cover. For each study year, a single Landsat scene was selected based on minimum cloud cover within the dry season window, with acquisition dates falling in June or July to ensure comparability across years.

All data processing was performed using the Google Earth Engine (GEE) cloud computing platform for large-scale computation and LULC classification [19]Spatial analysis and mapping were conducted in QGIS, and statistical processing was performed in Microsoft Excel.

Supporting spatial data used in this study include administrative boundary maps sourced from the Geospatial Information Agency (*Badan Informasi Geospasial*/BIG) and demographic and land-use statistics from the Central Bureau of Statistics (*Badan Pusat Statistik*/BPS) of West Sulawesi Province [1],[2]. These supporting datasets were used to delineate the study area and produce the maps presented in this research.

Preprocessing of ERA5 data included spatial extraction within the study area's bounding box and subsetting to the dry season period. Subsequently, the ERA5 data were converted from Kelvin to Celsius using the equation

$$T(°C) = T(K) - 273.15 \quad (1)$$

as well as outlier detection using the interquartile range (IQR) method.

For Landsat 8/9 data, preprocessing included cloud masking using the QA_PIXEL band with the CFMask algorithm [20]. as well as temporal synchronization with the ERA5 data over the same period. The Level-2 products used had already undergone standard USGS atmospheric and geometric corrections [21], making them ready for direct quantitative analysis.

Next, Land Surface Temperature (LST) was extracted from the Landsat 8/9 thermal band using standard USGS scale factors and offsets [22].

$$LST = (ST\_B10 \times 0.00341802 + 149.0) - 273.15 \quad (2)$$

where STB_10 is the Landsat surface temperature band value, 0.00341802 is the multiplicative rescaling factor, 149.0 is the additive rescaling factor, and 273.15 is the conversion constant from Kelvin to degrees Celsius [21].

To analyze the influence of vegetation and built-up areas on LST, two main spectral indices were calculated. First, NDVI was calculated to estimate vegetation density, which affects surface temperature. NDVI utilizes the difference in spectral response between the red band

(Red), which is absorbed by chlorophyll, and the near-infrared band (NIR), which is strongly reflected by leaf cell structures [23].

$$NDVI = \frac{NIR-Red}{NIR+Red} \quad (3)$$

Second, NDBI utilizes the difference in spectral response between the shortwave infrared (SWIR) and near-infrared (NIR) channels for built-up surfaces [24]. NDBI was calculated to identify built-up areas and measure urbanization intensity:

$$NDBI = \frac{SWIR-NIR}{SWIR+NIR} \quad (4)$$

The use of spectral indices such as NDVI and NDBI has proven effective in distinguishing vegetation cover and built-up areas [14],[15].

Table 1. Band Spectral Landsat 8/9

Band	Name	Wavelength (μm)	Primary Use
B2	Blue	0.45 – 0.51	Water penetration, aerosol analysis, bathymetry
B3	Green	0.53 – 0.59	Peak reflectance of green vegetation
B4	Red	0.64 – 0.67	Chlorophyll absorption, vegetation discrimination
B5	NIR	0.85 – 0.88	Biomass and vegetation vigor
B6	SWIR1	1.57 – 1.65	Soil and vegetation moisture
B7	SWIR2	2.11 – 2.29	Mineral discrimination, soil moisture

LULC classification was performed using the Random Forest algorithm with 200 decision trees in GEE [25], combining 6 spectral bands, 6 spectral indices, and 3 topographic variables (elevation, slope, hillshade) as inputs. Random Forest was selected for its robustness to multicollinearity, its resistance to overfitting through ensemble averaging, and its established effectiveness for land cover mapping from multispectral imagery [13]. The six land cover classes used were Water Body, Dense Forest/Vegetation, Agriculture, Shrub/Grassland, Bare Land, and Built-up Area. Training data were sourced from Copernicus Global Land Cover, validated through visual interpretation of high-resolution imagery, and supplemented by rule-based post-processing based on spectral index thresholds to improve classification accuracy [26].

Statistical analysis comprised three main components. First, UHI intensity was calculated as the difference between the average LST of urban and rural areas within the study area. Here, the urban zone represents the densely built-up core of Mamuju City (Mamuju District and Simboro District), while the rural zone encompasses the surrounding vegetated. The urban zone was operationally defined as pixels classified as Bare Land or Built-up Area, while the rural zone comprised all remaining classes (Water Body, Dense Forest/Vegetation, Agriculture, and Shrub/Grassland). The calculation is expressed as follows

$$\Delta T = T_{urban} - T_{rural} \quad (5)$$

This formula was then categorized according to the classification in Table 2 [27]. Second, the relationship between LST and air temperature, NDVI, and NDBI was analyzed using Pearson correlation coefficients, with interpretation provided in Table 3[28]. Third, land cover classification accuracy was evaluated using a confusion matrix with Overall Accuracy and Kappa Coefficient metrics as shown in Table 4 [29].

Table 2. UHI Intensity Classification [27]

UHI Intensity (ΔT)	Intensity level
< 2°C	Weak
2 – 4°C	Moderate
4 – 8°C	Strong
> 8°C	Very Strong

Table 3. Pearson Correlation Coefficient interpretation [28]

r Value	Interpretation
0.00 – 0.19	Very weak
0.20 – 0.39	Weak
0.40 – 0.59	Moderat
0.60 – 0.79	Strong
0.8 – 1.0	Very Strong

Table 4. Kappa Coefficient Interpretation [29]

κ Interval	Agreement level
< 0,00	Very poor
0.00–0.20	Poor
0.21–0.40	Fair
0.41–0.60	Moderate
0.61–0.80	Good
0.81–1.00	Very Good

The overall research workflow is presented in the following flowchart.

Result and Discussion

ERA5 Reanalysis data for the dry season (June–September) from 2015 to 2024 show an increasing trend in average air temperature in Mamuju City, from 27.01°C in 2015 to 27.21°C in 2024, with the highest value recorded in September 2024 at 27.69°C (Table 5). This increase of 0.2°C over one decade reflects a consistent accumulation of thermal pressure, along with the physical growth of the Mamuju City urban area, which drives increased anthropogenic activity and changes in land surface characteristics.

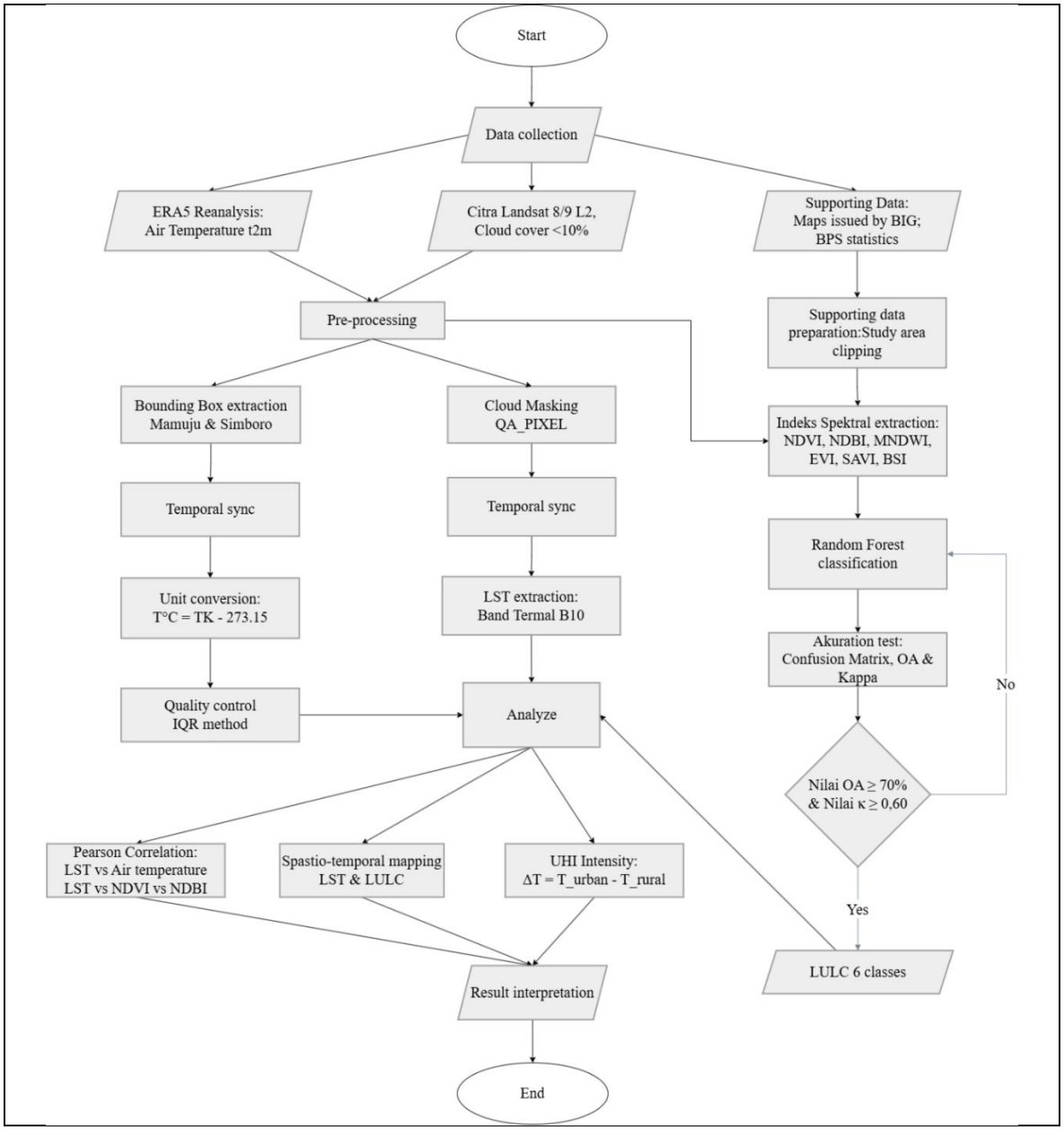

Figure 2. Research Flowchart of UHI Characteristics Analysis in Mamuju City

Table 5. Air Temperature in Mamuju City

Year	Air Temperature (°C)			
	June	July	August	September
2015	26.81	27.01	27.00	27.23
2016	27.06	27.11	27.47	27.18
2017	26.63	26.61	26.48	26.94
2018	26.66	26.90	26.95	27.14
2019	26.73	26.69	26.93	27.41
2020	26.66	26.35	27.10	26.59
2021	26.94	26.53	26.49	26.53
2022	26.55	26.70	26.68	26.53
2023	27.24	27.00	27.79	27.36
2024	26.93	27.20	27.01	27.69

In contrast to the relatively stable ERA5 air temperature signal, the LST data exhibit more fluctuating dynamics. Extraction results from 10 Landsat 8/9 scenes show an increase in average LST from 30.60°C in 2015 to 32.11°C in 2024, although not linear (Table 6). The spatial distribution shows high-temperature hotspots in the city center and along major road corridors, while vegetated areas consistently show lower temperatures (Figure 3).

Table 6. LST in Mamuju City

Image Date	LST (°C)			Std. Dev
	Min	Max	Mean	
26 Jun 2015	21.48	43.61	30.60	2.95
13 Jun 2016	20.43	48.83	33.47	3.52
16 Jun 2017	24.99	50.42	33.93	3.14
19 Jun 2018	24.00	47.07	32.98	3.36
08 Jul 2019	22.14	43.13	31.39	3.39
24 Jun 2020	15.07	44.71	30.63	5.46
29 Jul 2021	22.11	49.78	33.46	3.83
22 Jun 2022	17.43	44.39	29.39	3.63
27 Jul 2023	21.80	45.88	31.69	3.57
29 Jul 2024	21.13	47.43	32.11	3.66

Two temporal anomalies deviating from the trend should be noted. The highest LST value in 2017 (33.93°C) may partly reflect a lagged response to the strong 2015–2016 El Niño [30], which has been associated with moisture deficits and reduced vegetation cover, although single-scene acquisition precludes definitive attribution. Conversely, the lowest value in 2022 (29.39°C) coincides with the 2020 and 2022 La Niña phenomenon [30], which has been associated with above-normal rainfall and elevated atmospheric humidity. These associations are consistent with the broader role of ENSO as a short-term thermal modulator [31], though confirmatory analysis using multi-date dry season composites would strengthen causal attribution.

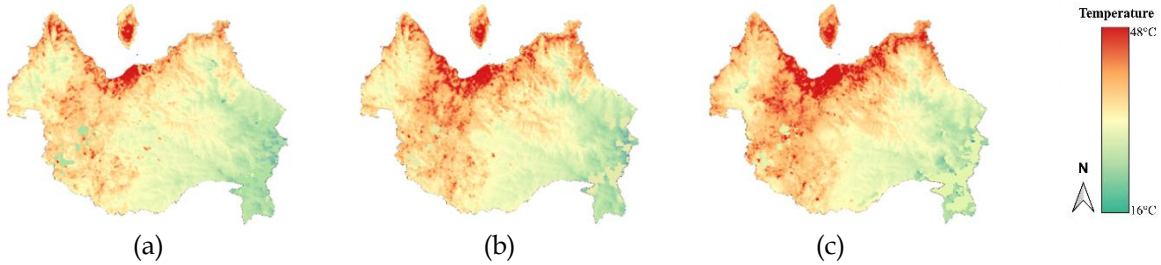

Figure 3. LST Distribution Map of Mamuju City: (a) 2015; (b) 2019; and (c) 2024

Spatially, the LST distribution map (Figure 3) shows that elevated surface temperatures are concentrated in the urban core and along infrastructure corridors, corresponding to the general spatial distribution of built-up areas extending from the urban center to the suburban areas, following infrastructure development and major road corridors. This conversion of vegetated land into impervious surfaces has direct thermal implications, as urban materials such as concrete and asphalt have much higher heat capacity and thermal emissivity than vegetation.

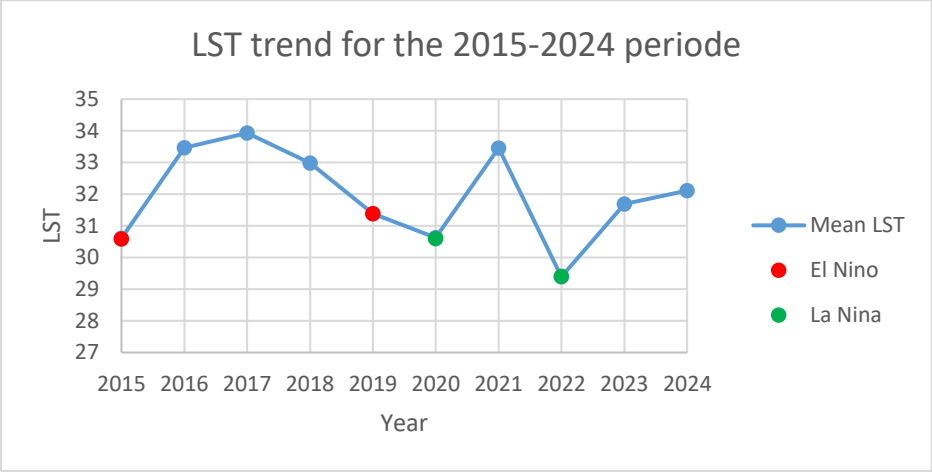

Figure 4. Average LST Trend for the 2015–2024 Period

Nevertheless, the long-term trend still shows a positive slope (Figure 4), confirming that land cover change due to urbanization is the main driver of LST increase, while ENSO acts as a temporal modulator. As indicated by the markers in Figure 4, El Niño years (red markers: 2015, 2019) are associated with above-normal LST relative to the trend, while La Niña years (green markers: 2020, 2022) are associated with below-normal LST, consistent with the known suppressive effect of La Niña on surface temperatures through increased rainfall and atmospheric humidity.

The observed changes in LST cannot be separated from the land-cover changes that occurred over the same period. Land cover classification using Random Forest with 200 decision trees and a 70/30 train-validation split yielded an Overall Accuracy of 71.96% and a Kappa Coefficient of 0.65, interpreted as good agreement. The results show that Dense

Forest/Vegetation decreased by 2,560.76 ha (7.92%), while Built-up Area increased by 610,0 ha (69.2%) over one decade (Table 7). The Kappa value indicates that the classification performs better than random assignment in distinguishing land cover types. However, the moderate overall accuracy suggests that certain land cover classes remain difficult to classify consistently.

Table 7. LULC Change in Mamuju City

LULC	Area (ha)			Change (ha)	Change (%)
	2015	2019	2024		
Water Bodies	860.96	571.19	570.00	−290.96	−33.79
Dense Forest/Vegetation	32,327.91	31,822.56	29,767.15	−2,560.76	−7.92
Agriculture	1,181.59	858.51	1,134.32	−47.27	−4.00
Shrub/Grassland	1,148.30	1,536.16	3,005.04	+1,856.74	+161.70
Bare Land	39.45	426.30	210.30	+170.85	+433.10
Built-up Area	881.60	1,225.21	1,491.64	+610.04	+69.20

The thermal consequences of these land cover changes are directly reflected in UHI intensity. To quantify this effect, the calculation of the LST difference between the urban zone (Bare Land + Built-up Area) and the rural zone (all other classes) shows that Mamuju City consistently falls into the Strong UHI category throughout the observation period.

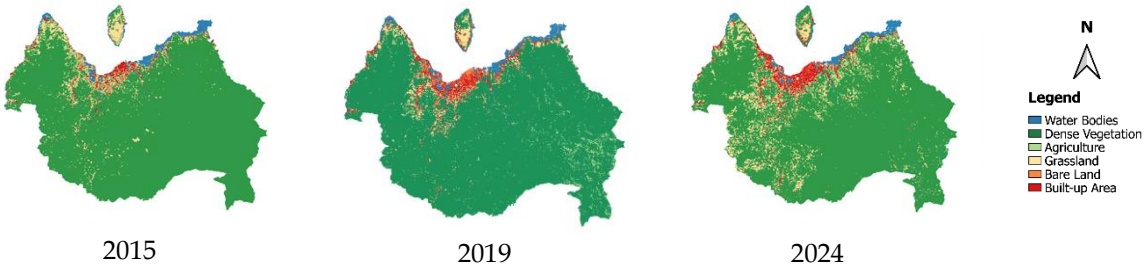

Figure 5. LULC change in Mamuju City: (a) 2015; (b) 2019; and (c) 2024

Figure 5 visually illustrates the land use and land cover (LULC) conditions in Mamuju City across three observation periods: 2015, 2019, and 2024. In 2015, the study area was still dominated by dense vegetation and agricultural land. By 2019, urban growth became apparent, particularly along major road corridors and coastal settlements, accompanied by a gradual decline in vegetation. In 2024, built-up and bare land areas expanded further and became more spatially connected, indicating a more advanced stage of urban expansion.

Building on these observations, spatial distribution shows that the highest UHI intensity tends to be concentrated in the urban core of Mamuju City, which directly correlates with the pattern of built-up area expansion observed in land cover change maps. The expansion occurs primarily along major road corridors, including Majene–Mamuju Main Road, Arteri Mamuju Artery Road, and the Manakarra beach reclamation area. This directional growth is driven by the availability of flat land suitable for residential and commercial development, as well as the

concentration of government facilities and public service centers that attract population influx from surrounding rural areas.

Table 8. UHI Intensity in Mamuju City

Year	LST Urban (°C)	LST Rural (°C)	ΔT (°C)	Category
2015	35.33	30.23	5.10	Strong
2016	39.48	32.93	6.55	Strong
2017	34.11	27.95	6.16	Strong
2018	38.99	32.49	6.49	Strong
2019	37.15	30.91	6.24	Strong
2020	37.22	30.11	7.11	Strong
2021	40.57	32.89	7.68	Strong
2022	38.46	32.13	6.34	Strong
2023	38.14	31.19	6.95	Strong
2024	38.79	31.62	7.18	Strong

Note: LST Urban = mean LST of pixels classified as Bare Land or Built-up Area (representing the urban core of Mamuju City: Mamuju District and Simboro District); LST Rural = mean LST of all remaining LULC classes (Dense Forest/Vegetation, Agriculture, Water Body, and Shrub/Grassland) within the study boundary.

The fluctuating pattern of UHI intensity in Mamuju City from 2015 to 2024 shows an upward trend. The trend line indicates a gradual increase despite slight decreases in 2017 (6.16°C) and 2022 (6.34°C). Two significant spikes are seen in 2021 (7.68°C) and 2024 (7.18°C), forming the highest peaks over the decade. Meanwhile, the lowest point occurred in 2015 (5.1°C). While interannual oscillations reflect climate variability, the upward trajectory of the trend line indicates that UHI intensity is progressively approaching the upper threshold of the Strong category, consistent with ongoing land cover change.

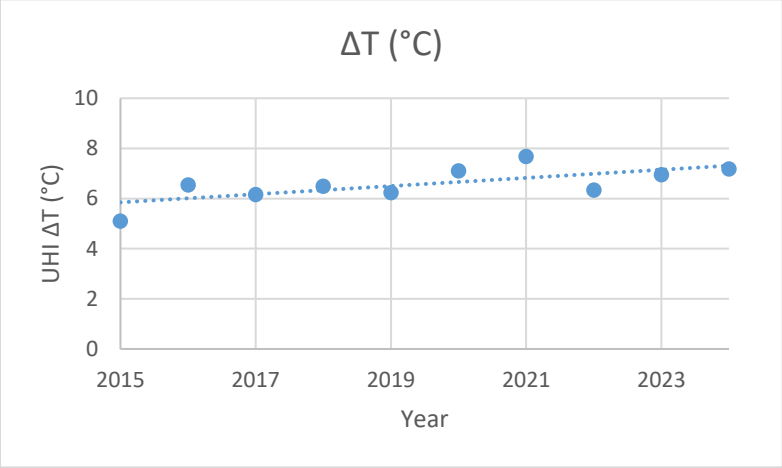

Figure 6. UHI Intensity trend in Mamuju City

Subsequently, LST derived from Landsat was compared with ERA5 air temperature at 10:00 WITA to match the satellite overpass time.

Table 9. LST and Air Temperature in Mamuju City at 10:00 WITA

Image Date	LST (°C)	Air Temperature (°C)
26 Jun 2015	30.60	26.7
13 Jun 2016	33.47	28.6
16 Jun 2017	33.93	26.7
19 Jun 2018	32.98	29.5
08 Jul 2019	31.39	28.9
24 Jun 2020	30.63	28.1
29 Jul 2021	33.46	29.5
22 Jun 2022	29.39	28.3
27 Jul 2023	31.69	30.0
29 Jul 2024	32.11	29.7

The correlation test between LST and air temperature yielded a very weak Pearson correlation coefficient (r) of 0.137 and was not significant ($p = 0.707$), indicating no statistically significant linear association (Tables 9 and 10). This result directly addresses one of the study's novel research objectives: whether coarse-resolution atmospheric reanalysis data can serve as a proxy for local surface thermal dynamics in a rapidly urbanizing tropical city. Based on this dataset, ERA5 air temperature at 0.25° spatial resolution does not serve as a reliable proxy for local LST variability at the city scale in Mamuju City. Physically, this outcome reflects the fundamental distinction between LST, which is a radiometric surface property that responds instantaneously to solar irradiance, surface albedo, and land cover type, and ERA5 air temperature, which represents a spatially smoothed, boundary-layer atmospheric mean integrated over a grid cell of approximately 25 km × 25 km at this latitude and is therefore far coarser than the intra-urban thermal gradients detectable at Landsat's 30 m resolution. The absence of a significant ERA5–LST relationship, therefore, has a practical implication for monitoring practice: ERA5 reanalysis data alone may be insufficient for characterizing intra-urban thermal heterogeneity at the city scale in Mamuju City. Consequently, satellite-derived thermal imagery plays an important role in resolving fine-scale thermal variability for spatially explicit urban heat assessment in rapidly urbanizing cities with limited ground-based observational networks.

Table 10. Pearson Correlation between LST and Air Temperature

Parameter	Value
Pearson Correlation Coefficient (r)	0.137
R^2	0.019
Significance (p-value)	0.707

Next, a Pearson correlation analysis of LST, NDVI, and NDBI was conducted across three periods (Tables 11–13). As similarly applied by Aldiansyah and Wardani [32], NDVI and NDBI values were extracted directly from Landsat 8/9 spectral bands at the pixel level and treated as continuous variables, given that both indices are inherently continuous in nature and are therefore more appropriately represented in numerical form to quantify their statistical relationship with LST.

Table 11. Correlation of LST, NDVI, and NDBI in 2015

Variable	r	R^2	p-value	Interpretation
LST vs NDBI	+0.701	0.491	<0.001	Strong Positive Correlation
LST vs NDVI	−0.658	0.433	<0.001	Strong Negative Correlation
NDBI vs NDVI	−0.867	0.751	<0.001	Strong Positive Correlation

Table 12. Correlation of LST, NDVI, and NDBI in 2019

Variable	r	R^2	p-value	Interpretation
LST vs NDBI	+0.721	0.518	<0.001	Strong Positive Correlation
LST vs NDVI	−0.693	0.481	<0.001	Strong Negative Correlation
NDBI vs NDVI	−0.886	0.785	<0.001	Strong Positive Correlation

Table 13. Correlation of LST, NDVI, and NDBI in 2024

Variable	r	R^2	p-value	Interpretation
LST vs NDBI	+0.662	0.439	<0.001	Strong Positive Correlation
LST vs NDVI	−0.680	0.462	<0.001	Strong Negative Correlation
NDBI vs NDVI	−0.897	0.805	<0.001	Strong Positive Correlation

The LST extracted from 10 Landsat 8/9 scenes reveals a progressive surface warming trend across Mamuju City, with a net increase over one decade. The thermal separation between urban and rural zones highlights that the built-up core is consistently warmer than surrounding vegetated areas. Peak urban LST corresponds to the highest UHI intensity during the observation period. Spatially, elevated surface temperatures concentrate in the urban core and along major infrastructure corridors, while vegetated zones act as localized thermal buffers, reflecting the influence of land cover on the local surface energy balance.

The strong negative relationship between LST and NDVI confirms that vegetation density is a primary determinant of surface temperature. Vegetated areas reduce surface warming through evapotranspiration and shading, while the reduction of Dense Forest/Vegetation by 2,560.76 ha likely diminishes the city's natural cooling capacity. The inter-annual variation in LST–NDVI correlation suggests that climatic variability, such as ENSO-driven moisture changes, modulates the cooling effect of vegetation over time.

The positive LST–NDBI correlation indicates that impervious surface density consistently drives higher surface temperatures. Urban materials, with lower albedo and limited evaporative capacity, amplify heat retention, while the expansion of built-up areas extends thermally elevated zones into previously vegetated regions. Inter-annual changes in the correlation may reflect evolving spatial heterogeneity of urban surfaces as the city develops.

The strong negative NDVI–NDBI correlation indicates that urban expansion primarily occurs at the expense of vegetated land, simultaneously reducing natural cooling and introducing heat-retaining surfaces, thereby sustaining high UHI intensity. This pattern, consistent with other urban studies, underscores the importance of preserving vegetation and managing impervious surfaces as key strategies for mitigating UHI in Mamuju City. The coastal tropical setting may further amplify thermal contrasts, highlighting the need for locally adapted urban planning.

Conclusion

Mamuju City has experienced a persistent and progressively strengthening Urban Heat Island phenomenon over the 2015–2024 period, consistently classified as Strong throughout the entire observation period. UHI intensity increased from 5.10°C in 2015 to 7.18°C in 2024, with the upward trend indicating that thermal pressure is approaching the upper threshold of the Strong category. This trajectory is primarily driven by the structural transformation of land cover, evidenced by the expansion of Built-up Area by 610.04 ha (+69.20%) and the contraction of Dense Forest/Vegetation by 2,560.76 ha (−7.92%) over the same decade.

The strong and statistically significant correlations between LST and both NDBI ($r = +0.662$ to $+0.721$) and NDVI ($r = -0.658$ to -0.693) across all three observation periods confirm that impervious surface expansion and vegetation loss are the dominant determinants of surface temperature variability in Mamuju City. ENSO variability, particularly El Niño and La Niña cycles, functions as a secondary temporal modulator, producing interannual fluctuations around the long-term warming trend without reversing its direction.

A key methodological finding of this study is that ERA5 reanalysis air temperature at 0.25° spatial resolution does not constitute a reliable proxy for local LST dynamics at the city scale, as evidenced by a very weak and statistically insignificant correlation ($r = 0.137$, $p = 0.707$). This result has direct practical implications: satellite-derived thermal imagery remains indispensable for spatially explicit UHI monitoring in rapidly urbanizing cities with limited ground-based observational infrastructure.

These findings provide an empirical spatial basis for UHI mitigation in Mamuju City. The spatial concentration of thermal hotspots along major road corridors and in the urban core, coinciding with areas of highest built-up density and lowest vegetation cover, identifies priority zones for targeted interventions, including urban green space preservation, impervious surface regulation in expansion areas, and vegetation-sensitive land-use planning. Future work should incorporate multi-date dry-season composites and Local Climate Zone classification to further resolve intra-urban thermal heterogeneity and strengthen causal attribution of observed LST dynamics.

Acknowledgment

The authors express their gratitude to their parents for providing full financial support, to Dr. Pariabti Palloan, S.Si., M.T., and Mr. Agus Susanto, S.Si., M.T., Ph.D., as supervisors, and to Mr. Adi Prasetyo for his technical assistance.

References

[1] Badan Pusat Statistik Provinsi Sulawesi Barat, *Sulawesi Barat Dalam Angka 2015*. Mamuju: BPS Provinsi Sulawesi Barat, 2015.

[2] Badan Pusat Statistik Provinsi Sulawesi Barat, *Sulawesi Barat Dalam Angka 2024*. Mamuju: BPS Provinsi Sulawesi Barat, 2024.

[3] S. N. Atsidiqy, E. H. Sujiyono, and Husain, "Modeling Influence of Urban Sprawl on Urban Heat Island (UHI) Activity in Kolaka Regency," *Indones. Phys. Rev.*, vol. 08, no. 01, pp. 162–180, 2025.

[4] U. S. EPA, "Heat Island Effect," United States Environtmental Protection Agency. [Online]. Available: https://www.epa.gov/heatislands. [Accessed: Jun. 2025].

[5] A. Dwivedi and R. Soni, "Impacts of urban heat island effect on critical urban infrastructure: a review of studies published between 2012 and 2022," *Environ. Rev.*, vol. 32, no. 4, pp. 457–469, 2024.

[6] F. Marsitha, W. J. Pattipeilohy, and R. H. Virgianto, "KENYAMANAN TERMAL KLIMATOLOGIS KOTA-KOTA BESAR DI PULAU SULAWESI BERDASARKAN TEMPERATURE HUMIDITY INDEX (THI)," *J. SAINTIKA UNPAM Vol. 1 No. 2 Januari 2019*, vol. 2, no. 2, pp. 175–183, 2020.

[7] M. Z. Alamsyah *et al.*, "Analisis Dampak ENSO terhadap Presipitasi dan Evaporasi di Selat Makassar," *Bul. Oseanografi Mar.*, vol. 14, no. 1, pp. 23–36, 2025.

[8] A. M. D. Asyam, B. Rochaddi, and R. Widiaratih, "Hubungan ENSO dan IOD terhadap Suhu Permukaan laut dan Curah Hujan Di Selatan Jawa Tengah," *Indones. J. Oceanogr.*, vol. 6, no. 2, pp. 165–172, 2024.

[9] A. H. Wali, R. Situmorang, and H. M. Taki, "Kajian Perkembangan Wilayah Provinsi Sulawesi Barat," *J. Bhuwana*, vol. 5, no. 1, pp. 32–40, 2025.

[10] I. Fardani and M. R. Yosliansyah, "Kajian Penentuan Prioritas Ruang Terbuka Hijau Berdasarkan Fenomena Urban Heat Island Di Kota Cirebon," *J. Sains Inf. Geogr.*, vol. 5, no. 2, p. 93, 2022.

[11] F. R. Fajary *et al.*, "Comprehensive spatiotemporal evaluation of urban growth, surface urban heat island, and urban thermal conditions on Java island of Indonesia and implications for urban planning," *Heliyon*, vol. 10, no. 13, p. e33708, 2024.

[12] M. D. Setiawati, M. P. Jarzebski, M. Gomez-Garcia, and K. Fukushi, "Accelerating Urban Heating Under Land-Cover and Climate Change Scenarios in Indonesia: Application of the Universal Thermal Climate Index," *Front. Built Environ.*, vol. 7, no. May, pp. 1–14, 2021.

[13] M. B. and L. Drăguţ, "'Random forest in remote sensing: A review of applications and future directions,'" *ISPRS J. Photogramm. Remote Sens.*, vol. 144, pp. 24–31, 2016.

[14] P. Rao, P. Tassinari, and D. Torreggiani, "Exploring the land-use urban heat island nexus under climate change conditions using machine learning approach: A spatio-temporal analysis of remotely sensed data," *Heliyon*, vol. 9, no. 8, p. e18423, 2023.

[15] S. T. Prasetyo, F. A. Rahman, S. Suryawati, S. Supriyadi, and E. Setiawan, "Land Use Analysis Using Machine-Learning Based on Cloud Computing Platform," *J. Ilmu Pertan. Indones.*, vol. 30, no. 4, pp. 765–772, 2025.

[16] and A. D. S. P. Sofan, K. I. N. Rahmi, N. M. Sari, J. T. Nugroho, T. Wati, "No Title"Modeling the surface thermal discomfort index (STDI) in a tropical environments using multi sensors: A case study of East Kalimantan, the future new capital city of Indonesia"," *J. Indian Soc. Remote Sens.*, vol. 52, no. 8, pp. 1761–1776, 2024.

[17] I. D. Stewart and T. R. Oke, "Local climate zones for urban temperature studies," *Bull. Am. Meteorol. Soc.*, vol. 93, no. 12, pp. 1879–1900, 2012.

[18] J. Muñoz-Sabater *et al.*, "ERA5-Land: A state-of-the-art global reanalysis dataset for land applications," *Earth Syst. Sci. Data*, vol. 13, no. 9, pp. 4349–4383, 2021.

[19] B. Kocaman and H. Ağaççıoğlu, "Assessment of the Impact of Land Use/Land Cover Changes on Carbon Emissions Using Remote Sensing and Deep Learning: A Case Study of the Kağıthane Basin," *Sustain.*, vol. 17, no. 23, pp. 1–24, 2025.

[20] B. F. Frimpong, A. Koranteng, and F. S. Opoku, "Analysis of urban expansion and its impact on temperature utilising remote sensing and GIS techniques in the Accra Metropolis in Ghana (1986–2022)," *SN Appl. Sci.*, vol. 5, no. 8, 2023.

[21] USGS, "Landsat Collection 2 Level-2 Science Products and related documentation," 2023. [Online]. Available: https://www.usgs.gov/landsat-missions/landsat-collection-2-level-2-science-products.

[22] M. Cook, J. R. Schott, J. Mandel, and N. Raqueno, "Development of an operational calibration methodology for the Landsat thermal data archive and initial testing of the atmospheric compensation component of a land surface temperature (LST) product from the archive," *Remote Sens.*, vol. 6, no. 11, pp. 11244–11266, 2014.

[23] C. Tucker, *Red and Photogrphic Infrared Linear Combinations for Monitoring Vegetation*, vol. 8. 1979.

[24] Z. Yong, J. Gao, and N. Shaoxiang, "Use of normalized difference built-up index in automatically mapping urban areas from TM imagery," *Int. J. Remote Sens.*, vol. 24, no. 3, pp. 583–594, 2003.

[25] S. Darmawan, R. Hernawati, and S. Rahmani, *Satellite-Based Urban Heat Island Study: A Prisma-Based Systematic Literature Review*, vol. 19, no. 6. 2025.

[26] M. Buchhorn *et al.*, "Copernicus Global Land Service: Land Cover 100m: Collection 3: epoch 2015: Globe (Version V3.0.1)," *Remote Sens.*, vol. 12, no. 6, p. 1044, 2020.

[27] T. R. Oke, "The energetic basis of the urban heat island," *Q. J. R. Meteorol. Soc.*, vol. 108, no. 455, pp. 1–24, 1982.

[28] J. D. Evans, *Straightforward Statistics for the Behavioral Sciences*. Pacific Grove, CA: Brooks/Cole Publishing, 1996.

[29] D. S. Shafer and Z. Zhang, Introductory Statistics. The Saylor Foundation, 2012. [Online]. Available: http://www.saylor.org/books.

[30] D. A. S. W. Betti Yuniasih, Wandi Nusa Harahap, "Anomali Iklim El Nino dan La Nina di Indonesia pada 2013-2022," *AGROISTA J. Agroteknologi*, vol. 6, no. 2, pp. 136–143, 2023.

[31] M. D. Y. Sopia Lestari, Jun-Ichi Hamada, Fadli Syamsudin, Sunaryo, Jun Matsumoto, "ENSO Influences on Rainfall Extremes around Sulawesi and Maluku Islands in the Eastern Indonesian Maritime Continent," *Sci. Online Lett. Atmos.*, vol. 12, no. 1, pp. 37–41, 2016.

[32] S. Aldiansyah and F. Wardani, "Analisis Spasio-Temporal Fenomena Urban Heat Island dan Hubungannya Terhadap Aspek Fisik di Kota Makassar (1993-2021)," *J. Sains Teknol. Modif. Cuaca*, vol. 24, no. 1, pp. 1–11, 2023.